Odontology (2024) 112:489–500
https://doi.org/10.1007/s10266-023-00868-z

ORIGINAL ARTICLE

Mechanical properties of simulated dentin caries treated with metal cations and L-ascorbic acid 2-phosphate

Mohammad Ali Saghiri[1,2,10] · Julia Vakhnovetsky[3,4] · Amir Abdolmaleki[6] · Elham Samadi[3,5] · Fatereh Samadi[3,5] · Salvatore Napoli[7] · Michael Conte[8] · Steven M. Morgano[9]

Received: 29 April 2023 / Accepted: 16 October 2023 / Published online: 17 November 2023

Abstract

This pH cycling study aimed to investigate the effects of L-Ascorbic acid 2-phosphate (AA2P) salts of Mg, Zn, Mn, Sr, and Ba on the surface microhardness, compressive strength, diametral tensile strength (DTS), and solubility of root canal dentin. 186 cylindrical dentin specimens from 93 teeth were fortified with optimal concentrations of AA2P salts of Mg (0.18 mM), Zn (5.3 µM), Mn (2.2×10^{-8} M), Sr (1.8 µM), and Ba (1.9 µM). Saline was used as the control group. These dentin specimens underwent a 3-day cycling process simulating dentin caries formation through repeated sequences of demineralization and remineralization. Surface microhardness at 100 and 500 µm depths ($n=10$/subgroup), scanning electron microscopy ($n=3$/group), compressive strength ($n=10$/group), DTS ($n=6$/group), and solubility ($n=5$/group) tests were performed to analyze the dentin specimens. Data were analyzed using Kolmogorov–Smirnov, one-way ANOVA, and Post Hoc Tukey tests ($p<0.05$). The control group had significantly lower microhardness at both depths ($p<0.001$), reduced DTS ($p=0.001$), decreased compressive strength ($p<0.001$), and higher weight loss ($p<0.001$) than all other groups. The Sr group had the highest compressive strength and microhardness among all the groups. The microhardness was significantly higher for the 500 µm depth than the 100 µm depth ($p<0.001$), but the difference in microhardness between depths across groups was not significant ($p=0.211$). All fortifying solutions provided some protection against artificial caries lesions. Therefore, these elements might have penetrated and reinforced the demineralized dentin against acid dissolution.

Keywords Demineralization · Dentin · Microhardness · pH cycling · Remineralization

Introduction

Dentin, a hard and slightly compressible oral tissue, contains approximately 70% inorganic elements, 20% organic elements, and 10% water [1]. It is characterized by long, thin tubules surrounded by inorganic peritubular dentin with a mineral content of over 90% [2, 3]. Dental caries is a prevalent pathological change of dentin driven by the disruption of the demineralization-remineralization balance by acidogenic bacteria [4–6]. Root dentin is particularly susceptible to caries development, with the rate of mineral loss being twice as fast as in enamel [7]. Although highly treated at

✉ Mohammad Ali Saghiri
saghiri@gmail.com

1 Department of Restorative Dentistry, Rutgers School of Dental Medicine, Newark, NJ, USA

2 Department of Endodontics, University of the Pacific, Arthur A. Dugoni School of Dentistry, San Francisco, CA, USA

3 Sector of Innovation in Dentistry, Dr. Hajar Afsar Lajevardi Research Cluster (DHAL), Hackensack, NJ, USA

4 University of Michigan School of Dentistry, Ann Arbor, MI, USA

5 Biomaterials Laboratory, Rutgers School of Dental Medicine, Newark, NJ, USA

6 Polydent Dental Materials Consulting, Victoria, Canada

7 Department of Oral & Maxillofacial Surgery, Rutgers School of Dental Medicine, Newark, NJ, USA

8 Department of Restorative Dentistry, Office of Clinical Affairs, Rutgers School of Dental Medicine, Newark, NJ, USA

9 Department of Restorative Dentistry, Rutgers School of Dental Medicine, Newark, NJ, USA

10 MSB C639A, Rutgers Biomedical and Health Sciences, 185 South Orange Avenue, Newark, NJ 07103, USA

early stages, caries can penetrate into deep tissues of the teeth, requiring a root canal to then restore the tooth [8]. Previous research demonstrated that carious dentin has reduced crystallinity and lower mineral content [9], with changes in magnesium levels indicating early demineralization and loss of the peritubular dentin matrix [10]. Clinically, carious dentin is softer than healthy dentin and exhibits lower tensile strength due to mineral loss in intertubular dentin [11–13]. Additionally, carious dentin shows histopathological changes that may lower bonding efficacy [14–16].

Evidence to date indicates that inorganic trace mineral levels affect dentin structure and mechanical properties, and ionic doping may drive such changes in dentin's hydroxyapatite crystalline matrix [$Ca_{10}(PO_4)_6(OH)_2$] [17–19]. To specifically investigate the impact of cation displacement, we focused on utilizing a large and safe anionic counterion, L-ascorbic acid-2-phosphate (AA2P). This choice was made because AA2P possesses a significantly low tendency for replacement due to its large size and is widely recognized for its biosafety, stability in aqueous solutions, and extensive applications in the food, pharmaceutical, and cosmetic industries [20, 21].

Despite sparse studies, findings suggest that trace elements such as strontium (Sr), barium (Ba), zinc (Zn), magnesium (Mg), and manganese (Mn) can significantly impact dentinal hydroxyapatite quality and reduce the occurrence of caries [17, 18, 22, 23]. Mg and Zn improve dentin mineralization [17, 24, 25], and Sr possesses antimicrobial properties and shows great potential in anti-caries treatment along with Ba [23, 26]. However, the role of Mn depends on the amount used and may either propagate or reduce caries [18, 27–30]. This provides support for the proposed study as well as a future method to control the physical properties of carious dentin with a fortified root canal irrigant.

The mineralization quality of dentin plays a significant role in determining its mechanical properties, with microhardness being a key indicator. Microhardness is considered crucial in assessing the initial signs of dentin caries and can indirectly detect changes in composition and surface structure, reflecting mineral gain or loss in dental hard tissues [11, 13, 31, 32]. Another commonly used method to evaluate mechanical response is the diametral tensile strength (DTS) test, which provides reproducible results and assesses the tensile strength of friable materials [33, 34]. Compressive strength, determined through a similar methodology as DTS but with different specimen orientations, is also important for characterizing mechanical properties, particularly in terms of tooth restoration and treatment longevity [35].

Previous studies on the mechanical properties of hydroxyapatite as a result of ionic doping have been done on synthetic hydroxyapatite instead of natural biological materials, and studies on natural materials mainly focused on bone and enamel [36–42]. In comparison, studies on dentin have been very limited [17–19, 43]. The present study aimed to evaluate the in vitro remineralization effect of five fortifying solutions (0.1 mol/L AA2P salts of Mg, Zn, Mn, Sr, and Ba, containing a large non-exchangeable anionic counterion of AA2P) on human premolar dentin caries. Surface microhardness, compressive strength, DTS, and solubility tests were conducted to evaluate the mechanical properties and demineralization resistance. Scanning electron microscopy (SEM) was performed to better understand the morphological changes on the dentin surface caused by the fortifying solutions. The null hypothesis was that no significant differences would be found between the saline and any of the tested fortifying solutions.

Materials and methods

Ethical considerations, inclusion and exclusion criteria

The Institutional Review Board approved the study protocol at Rutgers School of Dental Medicine (reference number 2021001753). 93 caries-free single-rooted premolars extracted for orthodontic purposes were included in this study. Teeth were collected from patients of both sexes between 20 and 40 years of age. Patients with a smoking history, a low-fat or vegetarian diet, or who were pregnant or lactating, were excluded from this study. Teeth were excluded from this study if they were preserved in antibacterial or fixative solutions, had cracks and defects (confirmed by using a stereomicroscope), or had previous root canal procedures or pathology. To disinfect the teeth, they were stored in 0.5% chloramine T at 4 °C for up to 15 days before use followed by storage in distilled water until tested.

Specimen size analysis

G*Power 3.1.9.2 (Heinrich-Heine-Universität Düsseldorf, Düsseldorf, Germany) detected the total specimen size based on an effect size of 0.59 and an alpha-type error of 0.05 to achieve a power of 0.90. For evaluation of compressive strength, 10 specimens were used in each group (saline, AA2P salts of Mg, Zn, Mn, Sr, and Ba) ($n = 10$/group). For the evaluation of microhardness, 20 specimens were used in each group ($n = 20$/group). Each group was further subdivided into two subgroups according to the indentation depth (μm): 100 and 500 ($n = 10$/subgroup).

For SEM evaluation, the specimen size was determined by using the results of a pilot study. By comparing the means and standard deviations for the six groups for color intensity (control: 0.00 ± 0.00; Mg: 9.9 ± 2.12; Zn: 7.35 ± 1.34; Ba: 5.55 ± 1.34; Sr: 6.2 ± 0.85; and Mn: 6.1 ± 0.71), we determined that the minimum number of samples in each group

was 2. The specimen size was increased by 30% to improve the validity of the study. Considering an alpha-type error of 0.05 and a power of 80% (effect size = 1.1), the final specimen size was estimated to be 3 per group for the unit of intensity test (G * Power 3.1.9.2; Heinrich-Heine-Universität Düsseldorf, Düsseldorf, Germany).

For the evaluation of solubility and DTS, the specimen size was also determined using the results of a pilot study. By comparing the means and standard deviations for the six groups for weight loss (control: 32.51 ± 3.06%; Mg: 12.61 ± 5.67%; Zn: 12.55 ± 3.82%; Ba: 18.96 ± 3.44%; Sr: 18.16 ± 4.21%; and Mn: 16.48 ± 4.55%) and DTS (control: 40.60 ± 3.37 Mpa; Mg: 57.60 ± 15.21 Mpa; Zn: 53.98 ± 9.94 Mpa; Ba: 61.96 ± 4.47 Mpa; Sr: 59.99 ± 1.91 Mpa; and Mn: 55.80 ± 11.56 Mpa), we determined that the minimum number of samples in each group was 4. The specimen size was increased by 20% to improve the validity of the study. Considering an alpha-type error of 0.05 and a power of 90%, the final specimen size was estimated to be 5 per group for solubility and 6 per group for DTS tests (G * Power 3.1.9.2; Heinrich-Heine-Universität Düsseldorf, Düsseldorf, Germany).

Specimen preparation

Routine access openings were prepared, and the working lengths were established 1 mm short of the apex. According to a previously described protocol [44], all of the canals were prepared up to file #35 with Protaper nickel-titanium rotary instruments (Dentsply-Maillefer, Ballaigues, Switzerland) and irrigated with 1% NaOCl while instrumenting the canals. Following root canal preparation, the canals were irrigated with 5 ml of 17% EDTA for 1 min and flushed with 5 ml of saline solution. 93 dentin discs with 6 mm thickness were obtained from the mid-root region using a low-speed Isomet diamond saw (Buehler, Lake Bluff, NY) under water cooling. To obtain a standardized flat surface, the dentin specimens were wet-ground with a 320-grit and polished with a 600-grit under continuous water irrigation. Two cylindrical specimens (4 × 6 mm) were then instrumented from each dentin disc using a 6 mm trephine bur (Trephine Drills Kit, China) [45]. A flow chart of the study design is shown in Fig. 1.

Cationic exchange

AA2P salts of the desired metals (optimal concentration based on their ability to exchange 20% of the initial amount in dentin: Mg (0.18 mM), Zn (5.3 µM), Mn (2.2×10^{-8} M), Sr (1.8 µM), and Ba (1.9 µM)) were prepared by the following method: 3.22 g of AA2P trisodium salt was dissolved in 30 mL of water. The solution was then passed through a column packed with 100 mL of a strongly acidic cationic exchange resin (a gel-type polystyrene resin having a sulfonic acid group as an ion-exchange group; Amberlite IR-120B, H + type), and the column was eluted with water to collect 150 mL of an effluent. The effluent was passed through a column packed with 120 mL of a weakly basic anionic exchange resin (a macroporous-type acrylic resin having a tertiary amine group as the ion-exchange group; Amberlite IRA-35) to obtain L-ascorbic acid only. The column was further developed with 150 mL of one of five metal chloride solutions (0.1 mol/L AA2P salts of Mg, Zn, Mn, Sr, and Ba) to obtain a fraction containing new cationic L-ascorbic acid 2 phosphates with Mg, Zn, Mn, Sr, or Ba [46] (Fig. 2).

The prepared dentin specimens were randomly divided into six groups according to the solution used. The canal of each section was covered with an adhesive wax at the lower surface of the dentin specimen. Dentin specimens were then irrigated with one of five intervening solutions (AA2P salts of Mg (0.18 mM), Zn (5.3 µM), Mn (2.2×10^{-8} M), Sr (1.8 µM), and Ba (1.9 µM)) for five minutes, with the saline solution used as the control group, as previously described [47]. The root canals were then flushed with 10 mL of distilled water immediately after each treatment to remove excess solution [43].

pH cycling

Fortified dentin specimens were subjected to a pH cycling procedure with repeated sequences of de/remineralization [48]. Artificial caries were formed in the dentin specimens by a 1-h immersion in 2.5 mL of demineralizing solution (1.5 mM $CaCl_2$, 0.9 mM KH_2PO_4, 50 mM acetate buffer, pH 4.8) (Sigma-Aldrich, St Louis, MO). All lesions were then immersed in 2.5 mL of remineralizing solution (1.5 mM $CaCl_2$, 0.9 mM KH_2PO_4, 20 mM HEPES [4-(2-hydroxyethyl)-1-piperazineethanesulfonic acid], pH 7.0) (Sigma-Aldrich, St Louis, MO) for 23 h. During each solution change, the specimens were rinsed with deionized water for 10 s. The pH cycling process was performed at 37℃ for three days.

Microhardness measurements

A Micro Met 5100 durometer microhardness tester (Buehler Ltd, Lake Bluff, IL) was used to measure the hardness of the fortified dentin specimens after exposure to a caries-inducing environment [49]. Each dentin specimen was further divided into two sections. Three separate indentations were made in each section at depths of 100 µm and 500 µm from the pulp–dentin interface using a 300-g load with a dwell time of 20 s for each measurement. The indentations were then evaluated under an optical microscope (Richter-Optica S850, China), and the average length of their two

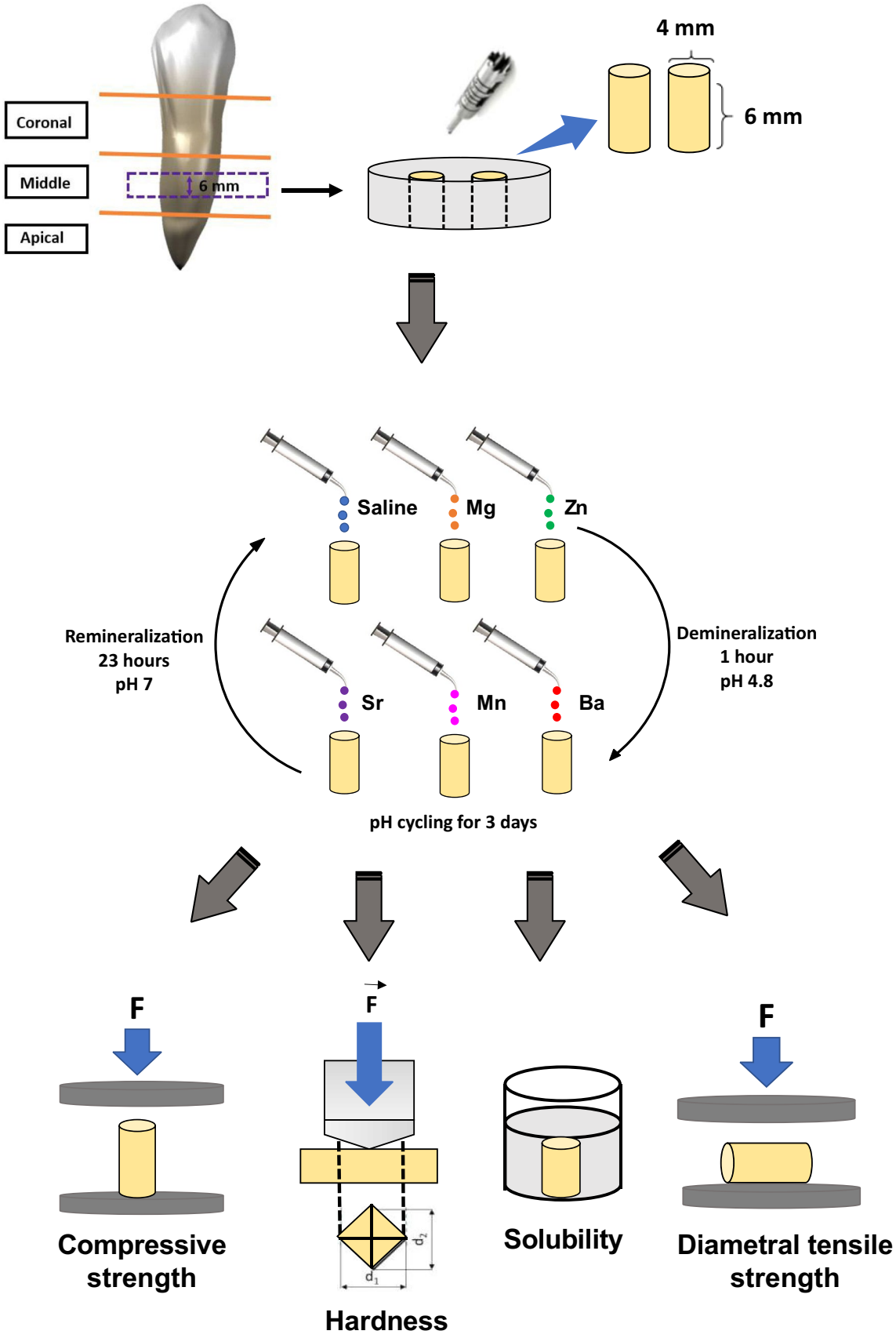

Fig. 1 Flowchart of the experimental design

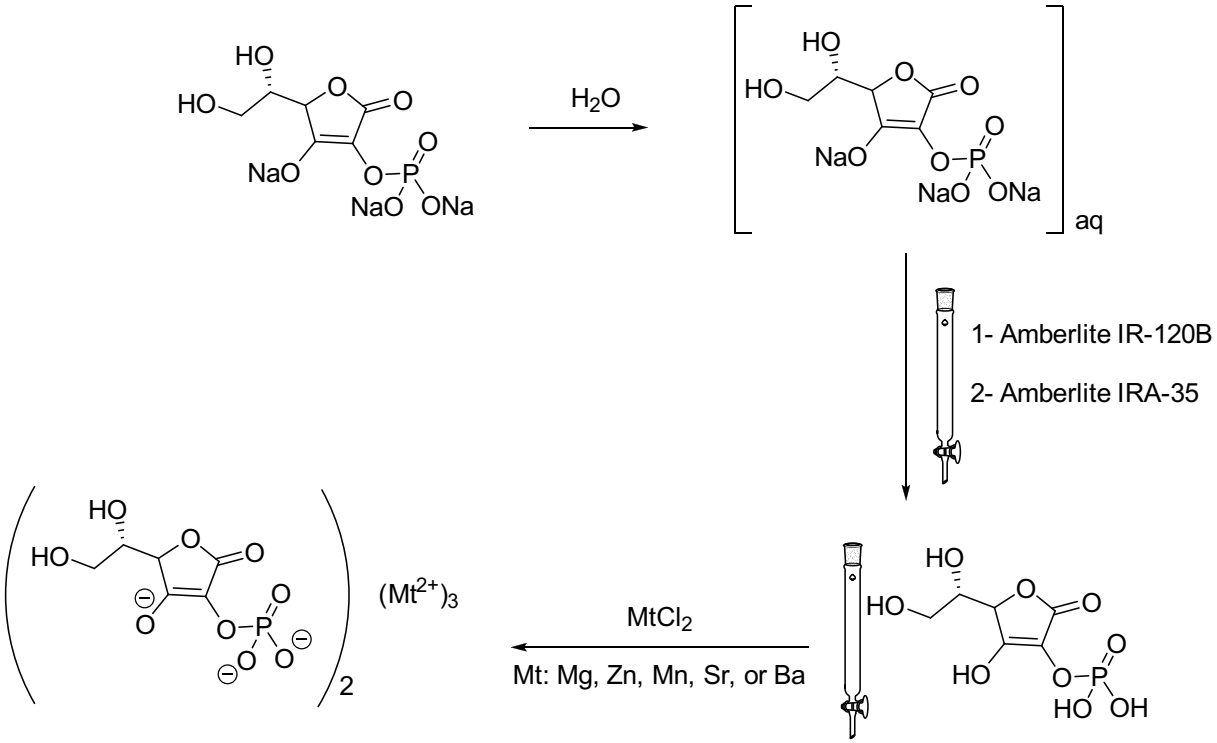

Fig. 2 Flowchart detailing the steps taken to make the cationic exchange solutions

diagonal lengths was used to determine the hardness. The average microhardness value of the indentations' results was considered representative of each depth in each specimen.

Scanning electron microscopy (SEM)

Three specimens from each group were examined by SEM–EDS mode to observe the precipitation of metallic components on the dentin surface [50]. All specimens were sectioned at a depth of 500 µm (exposure surface to fortifying solutions) using a diamond-coated disk under water cooling (Isomet 1000; Buehler). The specimens' surfaces were then polished and sputter-coated with 10 nm gold and observed under an SEM (VEGA; TESCAN, Brno, Czech Republic). EDS color dot map analysis was performed for each specimen at 1000X to evaluate the distribution of trace elements. The intensity of Mg, Zn, Mn, Sr, and Ba was measured using ImageJ (US National Institute of Health, Bethesda, MD) software. The color maps were converted to binary, and their mean color intensity (0 to 255 scale) was recorded as a unit of intensity (UI).

Diametral tensile strength (DTS)

The cylindrical specimens were positioned on a customized loading fixture to ensure that the 1.00-mm-diameter loading pin aligned with the center axis of the dentin cylinder. Additionally, flat platens were used at both ends of the specimens to further ensure alignment with the testing surface [45]. The specimens were then loaded horizontally into a universal testing machine (MTS 810, Eden Prairie, MN), receiving a uniaxial load perpendicular to their long axes and parallel to the dentinal tubule orientation. A 1.00-mm-diameter stainless steel plunger was used to apply downward pressure on the dentin surface at 1.0 mm/min crosshead speed. The maximal load applied to the plug at the time of dislodgement was recorded in Newtons, and the DTS was calculated using the formula $\sigma_d = \frac{2F}{\pi Dh}$, where F is the force in Newtons, D is the diameter of the cylinder, and h is the height in mm [51, 52].

Compressive strength

The procedure for compressive strength testing was the same as for DTS testing except for the orientation of the specimens in the universal testing machine (MTS 810, Eden Prairie, MN). The loads were applied uniaxially, parallel to the long axes of the specimens, and perpendicular to the dentinal tubule orientation until the specimens fractured. To calculate the compressive strength (MPa), the failure load (N) was divided by the area of the specimen in contact with the load $\left(\sigma c = \frac{F}{\pi r^2}\right)$.

Solubility evaluations

Fortified dentin specimens were completely immersed in 30 ml of 0.1 M butyric acid buffered with synthetic tissue fluid (pH 4.4) (Sigma–Aldrich, St Louis, MO) for 24 h at 37 °C and 100% humidity. After incubation, the specimens were removed from the acidic solutions, rinsed with distilled water to remove any residual acid, and dried. The weight of the dentin slices was measured by a digital microbalance (Optima High Precision Balance) before and after immersion into butyric acid, and the difference in weight informed us of dentin solubility [53].

Statistical analysis

Descriptive statistics were calculated for all outcomes. Normal distribution of the data was confirmed by the Kolmogorov–Smirnov test. One-way ANOVA was used to compare compressive strength, solubility, unit of intensity, and DTS among the six groups. A general linear model was performed to determine if the groups and depth affect the microhardness. Tukey HSD was used for the post hoc tests. IBM SPSS Statistics version 28.0 software (SPSS Inc., Chicago, IL) was used for all data analysis. The significance level (2-sided) was set to 0.05 for all tests.

Results

There was a significant difference in solubility among the groups ($p < 0.001$). The control group had significantly higher weight loss than all other groups (Fig. 3A). There was no significant difference between the non-control groups (Table 1).

There was a significant difference in DTS among the groups ($p = 0.001$). The control group had significantly lower DTS than all other groups (Fig. 3B). There was no significant difference between the non-control groups (Table 1).

There was a significant difference in compressive strength among the groups ($p < 0.001$). The control group had the lowest compressive strength and the Sr group had the highest compressive strength among all the groups (Fig. 3C). There was no significant difference among the Mg, Zn, Ba, and Mn groups, and between the Ba and Sr groups (Table 1).

In Table 2, the general linear model showed that the groups ($p < 0.001$) and depth ($p < 0.001$) significantly affected the microhardness. The control group had the lowest and the Sr group had the highest microhardness among all the groups. However, there was no significant difference between the Sr, Ba, and Mn groups. The microhardness for 500 µm depth was significantly higher than the one for 100 µm depth. The general linear model also showed that the interaction of groups and depth variables

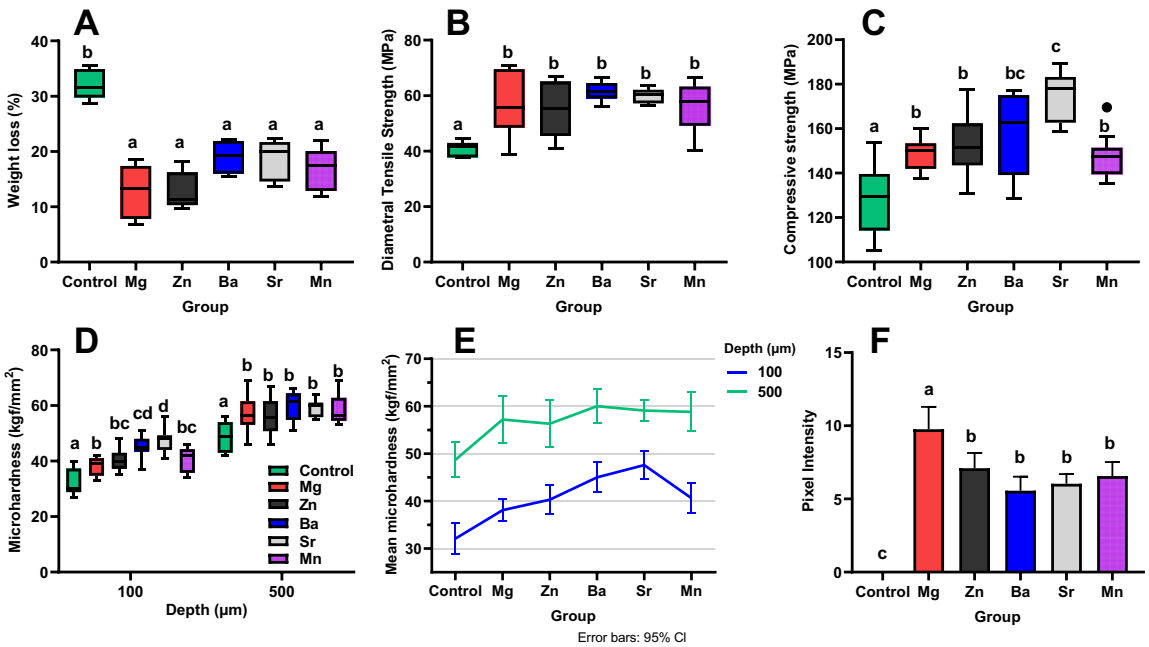

Fig. 3 **A** Box plots of the means and standard deviations showing the weight loss (%) for the six groups. **B** Box plots of the means and standard deviations showing the DTS (Mpa) for the six groups. **C** Box plots of the means and standard deviations show the compressive strength (Mpa) for the six groups. **D** Box plots of the means and standard deviations showing the surface microhardness at 100 and 500 µm depths for the six groups. **E** Mean and 95% confidence interval of microhardness for the groups by depth. **F** Pixel intensity of dentin specimens at 500 µm depth. *The different superscript letters in each column represent significant differences

Table 1 Descriptive statistics of DTS (Mpa), solubility (%), compressive strength (Mpa), and unit of intensity (UI) and comparison results between the groups

Groups	Mechanical properties			
	Diametral tensile strength	Solubility	Compressive strength	Unit of intensity
Control	40.99 ± 2.68^{a}	32.18 ± 2.75^{b}	127.21 ± 15.46^{a}	0.00 ± 0.00^{c}
Mg	56.93 ± 11.93^{b}	12.73 ± 4.92^{a}	148.97 ± 6.89^{b}	9.76 ± 1.52^{a}
Zn	54.97 ± 10.12^{b}	12.88 ± 3.39^{a}	152.40 ± 15.07^{b}	7.1 ± 1.04^{b}
Ba	61.56 ± 3.55^{b}	19.03 ± 2.99^{a}	157.96 ± 18.22^{bc}	5.57 ± 0.95^{b}
Sr	60.01 ± 2.70^{b}	18.53 ± 3.74^{a}	174.01 ± 11.09^{c}	6.03 ± 0.67^{b}
Mn	56.07 ± 9.39^{b}	16.69 ± 3.97^{a}	148.03 ± 9.82^{b}	6.57 ± 0.95^{b}

Different superscript letters indicate statistically significant differences between groups ($p < 0.001$, ANOVA and Tukey's HSD)

Table 2 Descriptive statistics of microhardness (kgf/mm^2) for the fortifying solutions and depth, and comparison results using a general linear model

	N	Mean	Std. deviation	*p*-value	Post hoc ** (Tukey HSD)
Groups					
Control	20	40.40	9.75	< 0.001*	a
Mg	20	47.65	11.11		b
Zn	20	48.30	9.96		bc
Ba	20	52.50	8.99		cd
Sr	20	53.35	6.87		d
Mn	20	49.70	10.59		bcd
Depth (µm)					
100	60	40.62	6.41	< 0.001*	
500	60	56.68	6.61		
Groups*depth				0.211	See Fig. 3

*The mean difference is significant at the 0.05 level

**Same letter means that the mean difference is not significant between the groups

Table 3 Descriptive statistics of microhardness (kgf/mm^2) for the groups by the depth and comparison results for each depth separately using one-way ANOVA

	N	Mean	Std. deviation	*p*-value	Post hoc ** (Tukey HSD)
100 µm depth					
Control	10	32.10	4.63	< 0.001*	a
Mg	10	38.10	3.18		b
Zn	10	40.30	4.24		bc
Ba	10	45.00	4.42		cd
Sr	10	47.60	4.12		d
Mn	10	40.60	4.48		bc
500 µm depth					
Control	10	48.70	5.10	< 0.001*	a
Mg	10	57.20	6.93		b
Zn	10	56.30	7.01		b
Ba	10	60.00	5.10		b
Sr	10	59.10	3.04		b
Mn	10	58.80	5.73		b

*The mean difference is significant at the 0.05 level

**Same letter means that the mean difference is not significant between the groups

was not significant ($p = 0.211$, Table 2), which means that the difference in microhardness between the two depths was not significantly different across the groups (Fig. 3E).

For the 100 µm depth, the microhardness was compared among the groups (Table 3). The result was similar to the combined data of 100 and 500 µm depth. The groups significantly affected the microhardness ($p < 0.001$). The control group had the lowest and the Sr group had the highest microhardness among all the groups. However, there was no significant difference between the Sr and Ba groups. For the 500 µm depth, the group variable was also significant ($p < 0.001$). The control group had significantly lower microhardness than all other groups. There was no significant difference between the non-control groups (Fig. 3D).

There was a significant difference in the unit of intensity among the groups for the SEM/EDS analyses ($p < 0.001$). The control group had the lowest intensity and the Mg group had the highest intensity among all the groups (Figs. 3F and 4a–e). There was no significant difference among the Zn, Mn, Sr, and Ba groups (Table 1).

Discussion

In the present study, we used a pH cycling model to evaluate the effect of different fortifying solutions on dentin caries by assessing changes in surface microhardness, DTS, compressive strength, and solubility, which may reflect the mechanical properties and degree of dentin demineralization. According to the results of this study, the null hypothesis was rejected.

The optimal duration for irrigating the specimens with each fortifying solution was determined based on our previous study measuring the physical properties of dentin

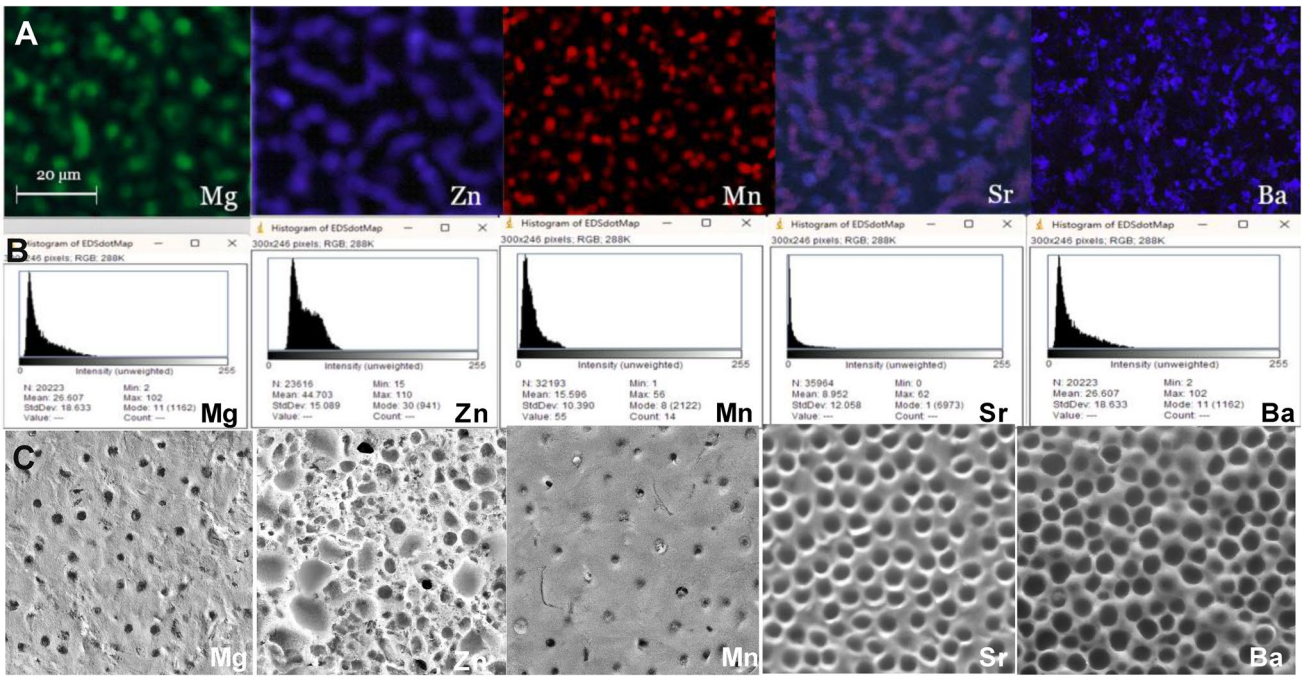

Fig. 4 **A** EDS dot map of dentin specimens at 1000× for (*a*) Mg; (*b*) Zn; (*c*) Mn; (*d*) Sr; and (*e*) Ba. **B** Histogram analysis of dentin specimens for (*a*) Mg; (*b*) Zn; (*c*) Mn; (*d*) Sr; and (*e*) Ba. **C** SEM images of dentin specimens at 1000× for (*a*) Mg; (*b*) Zn; (*c*) Mn; (*d*) Sr; and (*e*) Ba

(e.g., surface microhardness) after treatment with Mg, Sr, and Zn solutions [43]. Irrigation durations of 1, 2, 5, and 10 min were selected to align with the average time endodontic irrigants are used [54–56], as we aim to develop fortified irrigants for teeth in the future. The results demonstrated a time-dependent effect of these elements on dentinal properties, with a significant effect observed after 5–10 min. However, considering practical limitations in irrigant use, 5 min was chosen as the final irrigation time for the present study.

Dentin consists of many hydroxyapatite crystals with various cations and anions incorporated in its lattice, forming apatites with improved biomechanical properties [17–19]. To ensure that our experiments were not confounded by the substitution of anionic counterions, we considered the use of salts that have the same anionic counterion in the hydroxyapatite structure, such as hydroxide salts or phosphate ions. However, phosphates are insoluble and unsuitable for fortifying solutions/irrigants, while hydroxides are excessively basic, posing challenges in neutralizing the solutions and potentially leading to the formation of unwanted by-products. Another option is to utilize salts whose anionic counterions are very large and cannot be replaced in the hydroxyapatite structure. AA2P was selected due to its advantages over phosphates and hydroxides. In particular, as the size of the anionic counterion increases, displacement occurs solely through the exchange of the cation. As a result, the concentration gradient created by this displacement will eventually reach equilibrium, ultimately enhancing the penetration rate [57, 58].

Dentin specimens were treated with optimal concentrations of AA2P salts of Mg (0.18 mM), Zn (5.3 µM), Mn (2.2×10^{-8} M), Sr (1.8 µM), and Ba (1.9 µM)) for five minutes, with the saline solution used for the control group. The molarities of the AA2P salts were determined by taking into account the charge of the metal cation (+2) and the AA2P anion (− 3), resulting in an adequate molar solution for each metal. The cation and anion displacement ensured charge neutralization throughout the process.

The concentrations were selected to be 20% of the amount found in dentin to ensure uptake in dentin specimens while staying within the limits of the concentration safely allowable in the body [59–62]. Previous studies have demonstrated that increasing the concentration by 10–20% can improve bone tissue efficiency [57, 63], but, there are limits to the number of exchangeable surface elements, with a maximum of 30% for some elements [53]. Thus, 20% was considered an appropriate concentration for this study.

The present pH cycling model was previously suggested as a reliable method to simulate the acid-mediated demineralization process of root dentin and enamel surfaces [32, 48, 64, 65]. Dentin is more susceptible to caries than enamel due to factors such as a higher critical pH, faster demineralization, slower remineralization, and greater permeability to acids [66]. To account for the structural and compositional variations between enamel and dentin, the number of pH

cycles was reduced from 10 to 3. Moreover, the immersion time of the specimens in the demineralizing solution was shortened from 6 to 1 h, while the remineralizing solution exposure time was increased from 18 to 23 h [7, 48].

The degree of demineralization in artificial root caries lesions is typically evaluated using polarized light microscopy and microradiography [48, 67, 68]. However, polarized light microscopy provides only qualitative information, and microradiography is a destructive and time-consuming technique [69–72]. In this study, surface microhardness testing was selected because it reflects the initial signs of dentin caries [11, 13, 31], and can indirectly reveal mineral gain or loss in dental hard tissues by detecting changes in their composition and surface structure [32].

DTS is commonly used to evaluate the mechanical response of materials under diametrically applied stress due to its relative simplicity and reproducible results [33]. Additionally, it is the most widely used test for assessing the tensile strength of friable materials because it avoids the difficulties inherent to the flexural tensile strength test [34]. Compressive strength is also useful for characterizing mechanical properties and follows a similar methodology to DTS, except for the orientation of the specimens in the universal testing machine [35].

In the present study, dentinal mechanical properties, including surface microhardness, DTS, and compressive strength, were significantly lower in the control group compared to the Mg, Zn, Sr, Ba, and Mn groups. Lowered pH levels, below the critical range of 6.2–6.4 [73], can result in increased mineral content loss from dentin [74], which leads to reduced tensile strength and hardness [11–13]. Previous studies have also reported lower tensile strength in carious dentin compared to sound dentin, and a positive correlation between the tensile strength and hardness of carious dentin, which could be attributed to the weakened demineralized dentin matrix [12, 75].

The fortifying solutions used in this study, which contained Mg, Zn, Sr, Ba, or Mn, showed promising results in protecting against artificial caries lesions and improving the mechanical properties of carious dentin. The compressive strength and hardness varied significantly among the groups ($p < 0.001$), with the Sr group having the highest compressive strength and hardness and the control group having the lowest. This improvement in strength may be attributed to the conversion of hydroxyapatite into Sr apatite, which enhances acid resistance [76], and the remineralization of dentin tissue through newly formed apatite [77].

The Sr, Mg, Zn, Mn, and Ba groups had significantly higher DTS than the control group ($p = 0.001$), but no significant differences were found between them. The protective effect of fortifying solutions on carious dentin was attributed to the higher mechanical properties, which could be related to the stabilizing effect of Mg on amorphous calcium phosphate [78, 79] and the higher compressive strength, toughness, hardness, and density of Mn-doped hydroxyapatite compared to pure hydroxyapatite [28]. SEM analysis further confirmed that the metallic components of the fortifying solutions penetrated through the dentin to strengthen the tissue, with Mg exhibiting the highest penetration at the 500 µm depth (Fig. 4a–e).

Zn and Ba solutions also protected the dentin lesions in this study. These solutions significantly improved the surface microhardness at depths of 100 µm and 500 µm ($p < 0.001$), suggesting their ability to penetrate and strengthen the demineralized dentin against acid dissolution. Zn enhances the bioactivity and remineralization of dentin tissue by increasing Ca deposition and simulating protein phosphorylation and previously showed promising potential to treat radicular dentin with oxipatite, a zinc oxide-modified hydroxyapatite [17, 80]. Ba promotes greater remineralization and fracture healing in bone tissue, which may extend to dentin tissue as observed in this study, given the physiological and mechanical similarities between the two tissues [19, 42].

Solubility testing is a reliable and simple method for evaluating the chemical stability and susceptibility to demineralization of dental hard tissues, making it well-suited for investigating the effects of inorganic trace minerals on dentin solubility [53]. The present study used butyric acid for solubility testing to simulate the clinical conditions associated with dental caries formation, as it is a reported by-product of anaerobic bacterial metabolism [81–83]. Our results demonstrated that Mg, Sr, Zn, Ba, and Sr solutions provided 2–2.5 times greater resistance to dentin solubility than the saline solution. Mg increases the stability of dentin hydroxyapatite [84], while Zn promotes dentinal tubule occlusion through crystal precipitation that resists dental caries progression [80]. Sr may assist in achieving a balance between dentin demineralization and remineralization [17], whereas Mn and Ba, known to be involved in osteoblast proliferation, differentiation, and metabolism in bones [18, 42], may explain the lower solubility of carious dentin under low pH conditions in this study.

The limitations of this in vitro study include the absence of salivary and microbial influences that are typically present in natural caries lesions, as well as a relatively small specimen size. This study was also limited by the lack of a sound dentin control group, which could have provided information on whether the mineralizing treatments restored the baseline mechanical properties of dentin. Moreover, the study results only featured some of the properties that contribute to the potential effectiveness of AA2P salts as caries prevention agents. Future studies could explore the antibacterial activity and biocompatibility of AA2P salts, as well as use advanced characterization techniques such as atomic force microscopy and transverse microradiography to evaluate dentin surface roughness and mineral content, respectively.

Future directions for this research could include identifying the optimal combination of trace minerals and exposure times to achieve the desired mechanical properties of dentin. Furthermore, it would be interesting to investigate the effects of AA2P salts on soft tissues, such as the pulp cells and other cells in the vicinity, to assess their cytocompatibility and biological impact on periapical tissues.

Conclusion

Within the limitations of this study, all of the AA2P salts provided some protection against artificial caries lesions, suggesting that Mg, Zn, Sr, Ba, and Mn could have penetrated and strengthened the demineralized dentin against acid dissolution.

Acknowledgements MAS is a recipient of the DenburTech, New Jersey Health Foundation, NSF-DMR-2312680, NSF-STTR- 2321456, and TechAdvance Awards. This publication is dedicated to the memory of Dr. H. Afsar Lajevardi [85], a legendary pediatrician (1953–2015) who passed. We will never forget Dr. H Afsar Lajevardi's kindness and support. The views expressed in this paper are those of the authors and do not necessarily reflect the views or policies of the affiliated organizations. The authors hereby announce that they have active cooperation in this scientific study and preparation of the present manuscript. The authors confirm that they have no financial involvement with any commercial company or organization with direct financial interest regarding the materials used in this study. Special thanks to Shuying Jiang for interpreting the results of this research and Maziar Farhadi for all his help.

Declarations

Conflict of interest The authors deny any conflicts of interest related to this study.

References

1. Tjäderhane L, Carrilho MR, Breschi L, et al. Dentin basic structure and composition—an overview. Endod Topics. 2009;20(1):3–29.
2. Goldberg M, Kulkarni AB, Young M, et al. Dentin: structure, composition and mineralization: the role of dentin ECM in dentin formation and mineralization. Front Biosci (Elite Ed). 2011;3:711.
3. Purk JH. 8 - Morphologic and structural analysis of material-tissue interfaces relevant to dental reconstruction. In: Spencer P, Misra A, editors. Material-tissue interfacial phenomena. Woodhead Publishing; 2017. p. 205–29.
4. Lester K. Some preliminary observations in caries (" remineralization") crystals in enamel and dentine by surface electron microscopy. Virchows Arch Abt A Path Anat. 1968;344:196–212.
5. Kassebaum N, Bernabé E, Dahiya M, Bhandari B, Murray C, Marcenes W. Global burden of untreated caries: a systematic review and metaregression. J Dent Res. 2015;94(5):650–8.
6. Nakajima M, Kunawarote S, Prasansuttiporn T, Tagami J. Bonding to caries-affected dentin. Japan Dent Sci Rev. 2011;47(2):102–14. https://doi.org/10.1016/j.jdsr.2011.03.002.
7. Buzalaf MA, Hannas AR, Magalhães AC, Rios D, Honório HM, Delbem AC. pH-cycling models for in vitro evaluation of the efficacy of fluoridated dentifrices for caries control: strengths and limitations. J Appl Oral Sci. 2010;18(4):316–34. https://doi.org/10.1590/s1678-77572010000400002.
8. Bjørndal L, Laustsen MH, Reit C. Root canal treatment in Denmark is most often carried out in carious vital molar teeth and retreatments are rare. Int Endod J. 2006;39(10):785–90. https://doi.org/10.1111/j.1365-2591.2006.01149.x.
9. Spencer P, Wang Y, Katz JL, Misra A. Physicochemical interactions at the dentin/adhesive interface using FTIR chemical imaging. J Biomed Opt. 2005;10(3):031104–11.
10. Tjäderhane L, Hietala E-L, Larmas M. Mineral element analysis of carious and sound rat dentin by electron probe microanalyzer combined with back-scattered electron image. J Dent Res. 1995;74(11):1770–4.
11. Zheng L, Nakajima M, Higashi T, Foxton RM, Tagami J. Hardness and Young's modulus of transparent dentin associated with aging and carious disease. Dent Mater J. 2005;24(4):648–53.
12. Yoshiyama M, Tay F, Doi J, Nishitani Y, Yamada T, Itou K, et al. Bonding of self-etch and total-etch adhesives to carious dentin. J Dent Res. 2002;81(8):556–60.
13. Zheng L, Hilton JF, Habelitz S, Marshall SJ, Marshall GW. Dentin caries activity status related to hardness and elasticity. Eur J Oral Sci. 2003;111(3):243–52.
14. Erhardt MCG, Toledano M, Osorio R, Pimenta LA. Histomorphologic characterization and bond strength evaluation of caries-affected dentin/resin interfaces: effects of long-term water exposure. Dent Mater. 2008;24(6):786–98.
15. Wang Y, Spencer P, Walker MP. Chemical profile of adhesive/caries-affected dentin interfaces using Raman microspectroscopy. J Biomed Mater Res Part A: Off J Soci Biomater, Japan Soc Biomater, Aust Soc Biomater Korean Soc Biomater. 2007;81(2):279–86.
16. Perdigão J. Dentin bonding—variables related to the clinical situation and the substrate treatment. Dent Mater. 2010;26(2):e24–37. https://doi.org/10.1016/j.dental.2009.11.149.
17. Saghiri MA, Vakhnovetsky J, Vakhnovetsky A, et al. Functional role of inorganic trace elements in dentin apatite tissue—part 1: Mg, Sr, Zn, and Fe. J Trace Elem Med Biol. 2022;71:126932.
18. Saghiri MA, Vakhnovetsky J, Vakhnovetsky A. Functional role of inorganic trace elements in dentin apatite—part ii: copper, manganese, silicon, and lithium. J Trace Elem Med Biol. 2022. https://doi.org/10.1016/j.jtemb.2022.126995.
19. Saghiri MA, Vakhnovetsky J, Vakhnovetsky A, et al. Functional role of inorganic trace elements in dentin apatite tissue-part III: Se, F, Ag, and B. J Trace Elem Med Biol. 2022;72:126990. https://doi.org/10.1016/j.jtemb.2022.126990.
20. Zheng K, Song W, Sun A, Chen X, Liu J, Luo Q, et al. Enzymatic production of ascorbic acid-2-phosphate by recombinant acid phosphatase. J Agric Food Chem. 2017;65(20):4161–6. https://doi.org/10.1021/acs.jafc.7b00612.
21. Song W, Zheng K, Xu X, Gao C, Guo L, Liu J, et al. Enzymatic production of ascorbic acid-2-phosphate by engineered pseudomonas aeruginosa acid phosphatase. J Agric Food Chem. 2021;69(47):14215–21. https://doi.org/10.1021/acs.jafc.1c04685.
22. Liu X, Ma Y, Chen M, Ji J, Zhu Y, Zhu Q, et al. Ba/Mg co-doped hydroxyapatite/PLGA composites enhance X-ray imaging and bone defect regeneration. J Mater Chem B. 2021;9(33):6691–702.
23. Zdanowicz JA, Featherstone JD, Espeland MA, Curzon ME. Inhibitory effect of barium on human caries prevalence. Commun Dent Oral Epidemiol. 1987;15(1):6–9.
24. Ren F, Xin R, Ge X, Leng Y. Characterization and structural analysis of zinc-substituted hydroxyapatites. Acta Biomater. 2009;5(8):3141–9.
25. Tang Y, Chappell HF, Dove MT, Reeder RJ, Lee YJ. Zinc incorporation into hydroxylapatite. Biomaterials. 2009;30(15):2864–72.
26. Jayasree R, Kumar T, Mahalaxmi S, Abburi S, Rubaiya Y, Doble M. Dentin remineralizing ability and enhanced

antibacterial activity of strontium and hydroxyl ion co-releasing radiopaque hydroxyapatite cement. J Mater Sci - Mater Med. 2017;28(6):1–12.
27. Jelaca-Tavakoli M, Gerlach RF, Djuric M. Manganese (Mn) in human teeth. FASEB J. 2016;30:778–83.
28. Oliveira PH, Santana LAB, Ferreira NS, Sharifi-Asl S, Shokuhfar T, Shahbazian-Yassar R, et al. Manganese behavior in hydroxyapatite crystals revealed by X-ray difference Fourier maps. Ceram Int. 2020;46(8P):10585–97. https://doi.org/10.1016/j.ceramint.2020.01.062.
29. Mayer I, Jacobsohn O, Niazov T, Werckmann J, Iliescu M, Richard-Plouet M, et al. Manganese in precipitated hydroxyapatites. Eur J Inorg Chem. 2003;2003(7):1445–51.
30. Ghosh ANB, Kumar V, Nayan K. Role of minerals and trace elements in oral health - a review. J Oral Dent Health. 2016;2:1–2.
31. Pereira P, Inokoshi S, Yamada T, Tagami J. Microhardness of in vitro caries inhibition zone adjacent to conventional and resin-modified glass ionomer cements. Dent Mater. 1998;14(3):179–85.
32. Marquezan M, Corrêa FNP, Sanabe ME, Rodrigues Filho LE, Hebling J, Guedes-Pinto AC, et al. Artificial methods of dentine caries induction: a hardness and morphological comparative study. Arch Oral Biol. 2009;54(12):1111–7. https://doi.org/10.1016/j.archoralbio.2009.09.007.
33. Williams PD, Smith DC. Measurement of the tensile strength of dental restorative materials by use of a diametral compression test. J Dent Res. 1971;50(2):436–42. https://doi.org/10.1177/00220345710500025401.
34. Ban S, Anusavice K. Influence of test method on failure stress of brittle dental materials. J Dent Res. 1990;69(12):1791–9.
35. Davari A, Kazemi AD, Mousavinasab M, Yassaei S, Alavi A. Evaluation the compressive and diametric tensile strength of nano and hybrid composites. Dent Res J (Isfahan). 2012;9(6):827–8.
36. Talal A, Hamid SK, Khan M, et al. Structure of biological apatite: bone and tooth. In: Khan AS, Chaudhry AA, editors., et al., Handbook of ionic substituted hydroxyapatites. Cambridge: Woodhead Publishing; 2020. p. 1–19.
37. Palmer LC, Newcomb CJ, Kaltz SR, Spoerke ED, Stupp SI. Biomimetic systems for hydroxyapatite mineralization inspired by bone and enamel. Chem Rev. 2008;108(11):4754–83.
38. Tite T, Popa A-C, Balescu LM, Bogdan IM, Pasuk I, Ferreira JM, et al. Cationic substitutions in hydroxyapatite: current status of the derived biofunctional effects and their in vitro interrogation methods. Materials. 2018;11(11):2081.
39. Kay MI, Young R, Posner A. Crystal structure of hydroxyapatite. Nature. 1964;204(4963):1050–2.
40. Elliott J. Hydroxyapatite and nonstoichiometric apatites. Structure and chemistry of the apatites and other calcium orthophosphates. 1994;18:111-89
41. Šupová M. Substituted hydroxyapatites for biomedical applications: a review. Ceram Int. 2015;41(8):9203–31.
42. Ratnayake JTB, Mucalo M, Dias GJ. Substituted hydroxyapatites for bone regeneration: a review of current trends. J Biomed Mater Res B Appl Biomater. 2017;105(5):1285–99. https://doi.org/10.1002/jbm.b.33651.
43. Saghiri MA, Saghiri AM, Samadi E, et al. Neural network approach to evaluate the physical properties of dentin. Odontology. 2023;111(1):68–77. https://doi.org/10.1007/s10266-022-00726-4.
44. Saghiri MA, García-Godoy F, Asgar K, Lotfi M. The effect of Morinda Citrifolia juice as an endodontic irrigant on smear layer and microhardness of root canal dentin. Oral Sci Int. 2013;10(2):53–7. https://doi.org/10.1016/S1348-8643(12)00073-0.
45. Saghiri MA, Freag P, Nath D, Morgano SM. The effect of diabetes on the tensile bond strength of a restorative dental composite to dentin. Odontology. 2022. https://doi.org/10.1007/s10266-022-00697-6.
46. Shimbo K, Nagato N, Taguch I. Resonac Holdings Corp, Process for purifying L-ascorbic acid 2-phosphate,US06/892,013. 1988.
47. Saghiri MA, Delvarani A, Mehrvarzfar P, Malganji G, Lotfi M, Dadresanfar B, et al. A study of the relation between erosion and microhardness of root canal dentin. Oral Surg Oral Med Oral Pathol Oral Radiol Endodontol. 2009;108(6):e29–34.
48. Takeo Hara A, Silami de Magalhães C, Campos Serra M, Luiz RA. Cariostatic effect of fluoride-containing restorative systems associated with dentifrices on root dentin. J Dent. 2002;30(5):205–12. https://doi.org/10.1016/S0300-5712(02)00017-9.
49. Saghiri MA, Vakhnovetsky J, Dadvand S, et al. Impact of deproteinization methods on the physical and mechanical properties of dentin. Mater. 2022;25:101551. https://doi.org/10.1016/j.mtla.2022.101551.
50. Saghiri MA, Sheibani N, Kawai T, et al. Diabetes negatively affects tooth enamel and dentine microhardness: an in-vivo study. Arch Oral Biol. 2022. https://doi.org/10.1016/j.archoralbio.2022.105434.
51. Zaytsev D, Panfilov P. Deformation behavior of human dentin in liquid nitrogen: a diametral compression test. Mater Sci Eng, C. 2014;42:48–51. https://doi.org/10.1016/j.msec.2014.05.011.
52. Zaytsev D, Panfilov P. Deformation behavior of human enamel and dentin–enamel junction under compression. Mater Sci Eng, C. 2014;34:15–21. https://doi.org/10.1016/j.msec.2013.10.009.
53. Tadakamadla J, Kumar S, Ageeli A, Venkata Vani N, T MB. Enamel solubility potential of commercially available soft drinks and fruit juices in Saudi Arabia. Saudi J Dent Res. 2015;6(2):106–9. https://doi.org/10.1016/j.sjdr.2014.11.003.
54. Rath PP, Yiu CKY, Matinlinna JP, Kishen A, Neelakantan P. The effect of root canal irrigants on dentin: a focused review. Restor Dent Endod. 2020. https://doi.org/10.5395/rde.2020.45.e39.
55. Hülsmann M, Rödig T, Nordmeyer S. Complications during root canal irrigation. Endod Top. 2007;16(1):27–63.
56. Elbahary S, Haj-yahya S, Khawalid M, Tsesis I, Rosen E, Habashi W, et al. Effects of different irrigation protocols on dentin surfaces as revealed through quantitative 3D surface texture analysis. Sci Rep. 2020;10(1):22073. https://doi.org/10.1038/s41598-020-79003-9.
57. Ressler A, Žužić A, Ivanišević I, Kamboj N, Ivanković H. Ionic substituted hydroxyapatite for bone regeneration applications: a review. Open Ceram. 2021;6: 100122.
58. Uskoković V. Ion-doped hydroxyapatite: an impasse or the road to follow? Ceram Int. 2020;46(8):11443–65.
59. Cacciotti I. Cationic and anionic substitutions in hydroxyapatite. In: Antoniac IV, editor. Handbook of bioceramics and biocomposites. Cham: Springer International Publishing; 2016. p. 145–211.
60. Mehri A. Trace elements in human nutrition (II) - an update. Int J Prev Med. 2020;11:2. https://doi.org/10.4103/ijpvm.IJPVM_48_19.
61. Curtis EM, Cooper C, Harvey NC. Cardiovascular safety of calcium, magnesium and strontium: what does the evidence say? Aging Clin Exp Res. 2021;33(3):479–94. https://doi.org/10.1007/s40520-021-01799-x.
62. (ATSDR) AfTSaDR. Toxicological profile for Barium. Department of Health and Human Services, Public Health Service, Atlanta, GA: US. 2007. https://wwwn.cdc.gov/TSP/PHS/PHS.aspx?phsid=325&toxid=57#:~:text=NIOSH%20considers%20exposure%20to%20barium,dangerous%20to%20life%20or%20health. Accessed 16 Jun 2023.
63. Jiang Y, Yuan Z, Huang J. Substituted hydroxyapatite: a recent development. Mater Technol. 2020;35(11–12):785–96. https://doi.org/10.1080/10667857.2019.1664096.
64. ten Cate JM, Buijs MJ, Miller CC, Exterkate RAM. Elevated fluoride products enhance remineralization of advanced enamel lesions. J Dent Res. 2008;87(10):943–7. https://doi.org/10.1177/154405910808701019.

65. Lagerweij MD, ten Cate JM. Acid susceptibility at various depths of pH-cycled enamel and dentine specimens. Caries Res. 2006;40(1):33–7. https://doi.org/10.1159/000088903.
66. ten Cate JM, Buijs MJ, Damen JJ. pH-cycling of enamel and dentin lesions in the presence of low concentrations of fluoride. Eur J Oral Sci. 1995;103(6):362–7. https://doi.org/10.1111/j.1600-0722.1995.tb01858.x.
67. Wang Y, Xiong K, Chen X, Chi Y, Han Q, Zou L. The remineralization effect of germ clean on early human enamel caries lesions in vitro. Sci Rep. 2023;13(1):4178. https://doi.org/10.1038/s41598-023-31405-1.
68. Creanor S, Awawdeh L, Saunders W, Foye R, Gilmour W. The effect of a resin-modified glass ionomer restorative material on artificially demineralised dentine caries in vitro. J Dent. 1998;26(5–6):527–31.
69. Serra MC, Cury JA. The in vitro effect of glass-ionomer cement restoration on enamel subjected. Quintessence Int. 1992;23:143–7.
70. Featherstone J, Ten Cate J, Shariati M, Arends J. Comparison of artificial caries-like lesions by quantitative microradiography and microhardness profiles. Caries Res. 1983;17(5):385–91.
71. Lo E, Zhi Q, Itthagarun A. Comparing two quantitative methods for studying remineralization of artificial caries. J Dent. 2010;38(4):352–9.
72. Al-Obaidi R, Salehi H, Desoutter A, Bonnet L, Etienne P, Terrer E, et al. Chemical & nano-mechanical study of artificial human enamel subsurface lesions. Sci Rep. 2018;8(1):4047. https://doi.org/10.1038/s41598-018-22459-7.
73. Heijnsbroek M, Paraskevas S, Van der Weijden G (2007) Fluoride interventions for root caries: a review. Oral health & preventive dentistry 5(2):145–152.
74. Abou Neel EA, Aljabo A, Strange A, Ibrahim S, Coathup M, Young AM, et al. Demineralization–remineralization dynamics in teeth and bone. Int J Nanomed. 2016;11:4743.
75. Nishitani Y, Yoshiyama M, Tay FR, Wadgaonkar B, Waller J, Agee K, et al. Tensile strength of mineralized/demineralized human normal and carious dentin. J Dent Res. 2005;84(11):1075–8. https://doi.org/10.1177/154405910508401121.
76. Ito S, Iijima M, Hashimoto M, Tsukamoto N, Mizoguchi I, Saito T. Effects of surface pre-reacted glass-ionomer fillers on mineral induction by phosphoprotein. J Dent. 2011;39(1):72–9.
77. Dai LL, Mei ML, Chu CH, Lo ECM. Remineralizing effect of a new strontium-doped bioactive glass and fluoride on demineralized enamel and dentine. J Dent. 2021;108: 103633.
78. Yu T, Ye J, Zhang M. Effect of magnesium doping on hydration morphology and mechanical property of calcium phosphate cement under non-calcined synthesis condition. J Am Ceram Soc. 2013;96(6):1944–50. https://doi.org/10.1111/jace.12235.
79. Bigi A, Boanini E, Gazzano M (2016) Ion substitution in biological and synthetic apatites. Biomineralization and Biomaterials 235–66
80. Osorio R, Osorio E, Cabello I, Toledano M. Zinc induces apatite and scholzite formation during dentin remineralization. Caries Res. 2014;48(4):276–90.
81. Tonetti M, Cavallero A, Botta GA, Niederman R, Eftimiadi C. Intracellular pH regulates the production of different oxygen metabolites in neutrophils: effects of organic acids produced by anaerobic bacteria. J Leukoc Biol. 1991;49(2):180–8.
82. Saghiri MA, Lotfi M, Saghiri AM, Vosoughhosseini S, Fatemi A, Shiezadeh V, et al. Effect of pH on sealing ability of white mineral trioxide aggregate as a root-end filling material. J Endod. 2008;34(10):1226–9. https://doi.org/10.1016/j.joen.2008.07.017.
83. Shokouhinejad N, Nekoofar MH, Iravani A, Kharrazifard MJ, Dummer PM. Effect of acidic environment on the push-out bond strength of mineral trioxide aggregate. J Endod. 2010;36(5):871–4. https://doi.org/10.1016/j.joen.2009.12.025.
84. Andrés NC, D'Elía NL, Ruso JM, AnE C, Massheimer VL, Messina PV. Manipulation of Mg2+–Ca2+ switch on the development of bone mimetic hydroxyapatite. ACS Appl Mater Interfaces. 2017;9(18):15698–710.
85. Saghiri MA, Saghiri A. In Memoriam: Dr. Hajar Afsar Lajevardi MD, MSc, MS (1955–2015). Iran J Pediatr. 2017. https://doi.org/10.5812/ijp.8093.